

Calculation of second-order optical response in semiconductors

James L. P. Hughes and J. E. Sipe

Department of Physics, University of Toronto, Toronto, Ontario, Canada M5S 1A7

(Received 21 December 1995)

We present a first-principles calculation of two second-order optical response functions as well as the dielectric function for GaAs and GaP. Specifically, we evaluate the dielectric function $\epsilon(\omega)$ and the second-harmonic generation response coefficient $\chi^{(2)}(-2\omega; \omega, \omega)$ over a large frequency range. The electronic linear electro-optic susceptibility $\chi^{(2)}(-\omega; \omega, 0)$ is also evaluated below the band gap. These results are based on a series of self-consistent LDA calculations using the full-potential linearized augmented plane wave method. Self-energy corrections are included at the level of the “scissors” approximation, which corrects for the underestimation of the local density approximation band gap and produces a change in the velocity matrix elements. The analytic expressions for the second-order response functions are free of the unphysically divergent terms at zero frequency that have previously plagued such calculations. Results for $\chi^{(2)}(-\omega; \omega, 0)$ are in good agreement with experiment below the band gap and those for $\chi^{(2)}(-2\omega; \omega, \omega)$ are compared with experimental data where available. We note that despite the equivalence of both of these second-order response functions at zero frequency, there seems to be some discrepancy between the experimental results for these functions in this regime.

I. INTRODUCTION

While there have been many empirical and *ab initio* full band structure calculations of linear optical response in semiconductors,¹⁻⁹ there have been very few calculations of the nonlinear response. The understanding and calculation of the linear electro-optic (LEO) susceptibility has lagged behind the experimental studies, with most theoretical calculations based on simple phenomenological models.¹⁰⁻¹² Of the other second-order susceptibilities, most theoretical calculations have been concerned with second-harmonic generation (SHG),^{13,14} and many of these have been restricted to a determination of the response function at zero frequency.¹⁵⁻¹⁹ To our knowledge the only attempts at calculating nonlinear response functions over a wide frequency range are the work of Huang and Ching²⁰⁻²² and that of Moss and co-workers.²³⁻²⁷ As we discuss below, both of these approaches have certain limitations.

In this paper we present the results for the SHG and LEO response functions, as well as the dielectric function for GaAs and GaP over a wide frequency range. Since our interest is in the electronic aspects of optical response, we calculate the LEO response function in the “clamped lattice” approximation; our results are then suitable for comparison with experiments involving “dc-like” fields at low enough frequencies that electronic dispersion associated with the dc-like field can be neglected, but at high enough frequencies that lattice motion can be considered frozen out.

The analytic expressions for the nonlinear response functions are based on the formalism of Sipe and Ghahramani,²⁸ as extended and developed in the length gauge by Aversa and Sipe;²⁹ the response calculation is at the level of the independent particle approximation. This approach has the advantage that the response coefficients are inherently free of any unphysical divergences at zero frequency, a consequence of a careful treatment and separation of interband and intraband motion. “Sum rules” are not required to eliminate ar-

tificial divergences. The recent work of Dal Corso and Mauri,³⁰ based on an elegant Wannier function approach, is also free of such divergences. But at finite frequency, in particular, for frequencies or frequency sums across the gap, we feel that any approach easily amenable to numerical analysis will likely involve a \mathbf{k} -space focus such as that adopted explicitly in this work, simply because the resonances at any given frequency occur in localized regions of \mathbf{k} space.

The full band structure calculation in this work utilizes the full-potential linearized augmented plane wave (FLAPW) method^{31,32} within the local density approximation (LDA). This method has an advantage over that employed by Moss and co-workers²³⁻²⁷ in that it is first principles rather than semiempirical in nature. We have adopted a “scissors” approximation to correct for the band gap, but account for the change in the velocity matrix elements that appear in the response function expressions. Huang and Ching²⁰⁻²² neglect this modification in the matrix elements; based on previous evidence,¹⁸ and the results of our own calculations, this can result in a significant error in the determination of the response functions. We have not included local field effects in this work; as suggested by the work of Levine and Allan,¹⁸ we do not expect significant corrections for the materials considered here at the level of second-order response. However, the inclusion of local field effects can be done in a straightforward way within our formalism for the response functions.

The paper is organized in the following way. In Sec. II we present the analytic expressions for the linear and nonlinear response functions, and discuss the scissors approximation and its implementation. We outline the FLAPW method and the calculational technique used in determining the nonlinear coefficients in Sec. III. The band structures for the materials considered are also presented in this section. In Sec. IV we give our results for linear response, the SHG coefficient, and the LEO function. The comparison with experiment and

other theoretical calculations is also investigated and discussed. A conclusion and summary of our results are presented in Sec. V.

II. ANALYTIC EXPRESSIONS FOR OPTICAL RESPONSE

A. Response functions

We begin with results that follow directly from the independent particle approximation; in the following subsection we describe the modifications that must be made to implement the ‘‘scissors’’ approximation.

To establish our convention for the optical susceptibilities, we define the electric field and the polarization in terms of their frequency components as

$$\mathbf{E}(t) = \sum_n \mathbf{E}(\omega_n) e^{-i\omega_n t}, \quad (1)$$

$$\mathbf{P}(t) = \sum_n \mathbf{P}(\omega_n) e^{-i\omega_n t}, \quad (2)$$

where the summation extends over positive and negative frequencies ω_n . We adopt the convention that a zero-frequency component is to be included twice in the sums of Eqs. (1) and (2); then $2\mathbf{E}(0)$ is the actual value of the dc electric field. For completeness and clarity, we discuss matters of convention and definition in more detail in Appendix A.

At the level of linear response the polarization is given in terms of the electric field by²⁸

$$P^a(\omega) = \chi_I^{ab}(-\omega; \omega) E^b(\omega), \quad (3)$$

where superscripts indicate Cartesian components and are to be summed over if repeated; the linear susceptibility is given by

$$\chi_I^{ab}(-\omega; \omega) = \frac{e^2}{\Omega \hbar} \sum_{nm\mathbf{k}} f_{nm} \frac{r_{nm}^a(\mathbf{k}) r_{mn}^b(\mathbf{k})}{\omega_{mn}(\mathbf{k}) - \omega}. \quad (4)$$

Here and below n, m , etc., label energy bands; $f_{mn} \equiv f_m - f_n$, with f_i the Fermi occupation factor which, for the clean, cold semiconductors we study here, is zero or unity. The wave vectors \mathbf{k} range over the Brillouin zone, spaced as required by the normalization volume Ω . The factor of two to account for spin degeneracy is not included in Eq. (4) or any subsequent equation involving a summation over \mathbf{k} ; spin degeneracy is accounted for in all expressions below where the summation over \mathbf{k} has been converted to an integral. The frequency differences $\omega_{mn}(\mathbf{k}) \equiv \omega_m(\mathbf{k}) - \omega_n(\mathbf{k})$, where $\hbar \omega_n(\mathbf{k})$ is the energy of band n at wave vector \mathbf{k} ; frequencies ω such as that appearing in the denominator of Eq. (4) should be interpreted as $\omega + i0^+$, where 0^+ is a small positive quantity that is allowed to vanish at the end of the calculation. Finally, the \mathbf{r}_{mn} are the matrix elements of the position operator, excluding the diagonal part; for $\omega_{nm} \neq 0$ we have

$$r_{nm}^a(\mathbf{k}) \equiv \frac{v_{nm}^a(\mathbf{k})}{i\omega_{nm}}, \quad (5)$$

where $v_{nm}^a(\mathbf{k}) = m^{-1} p_{nm}^a(\mathbf{k})$, m is the free electron mass, and \mathbf{p}_{nm} is the indicated momentum matrix element.

The dielectric function $\epsilon^{ab}(\omega) \equiv 1 + 4\pi \chi_I^{ab}(-\omega; \omega)$, and so the usual expression for the imaginary part of $\epsilon^{ab}(\omega)$, $\epsilon_2^{ab}(\omega)$, follows from Eq. (4),

$$\epsilon_2^{ab}(\omega) = \frac{e^2}{\hbar \pi} \sum_{nm} \int d\mathbf{k} f_{nm} \frac{v_{nm}^a(\mathbf{k}) v_{mn}^b(\mathbf{k})}{\omega_{mn}^2} \delta(\omega - \omega_{mn}(\mathbf{k})), \quad (6)$$

where we have converted to an integral over the Brillouin zone.

For the second-order response we generally follow the susceptibility convention of Boyd.³³ Then a nonlinear polarization component is related to the electric field by

$$P^a(\omega_\beta + \omega_\gamma) = \chi^{abc}(-\omega_\beta - \omega_\gamma; \omega_\beta, \omega_\gamma) E^b(\omega_\beta) E^c(\omega_\gamma), \quad (7)$$

where χ^{abc} indicates the second-order susceptibility. Cartesian components are again summed over if repeated, as are frequency components ω_β and ω_γ , but only such that the sum $(\omega_\beta + \omega_\gamma)$ is held fixed; the susceptibilities are taken to satisfy intrinsic permutation symmetry $\chi^{abc}(-\omega_\beta - \omega_\gamma; \omega_\beta, \omega_\gamma) = \chi^{acb}(-\omega_\beta - \omega_\gamma; \omega_\gamma, \omega_\beta)$. In the specific case of second-harmonic generation we have

$$P^a(2\omega) = \chi^{abc}(-2\omega; \omega, \omega) E^b(\omega) E^c(\omega), \quad (8)$$

while for the linear electro-optic susceptibility we have

$$P^a(\omega) = 2\chi^{abc}(-\omega; \omega, 0) E^b(\omega) E_{dc}^c, \quad (9)$$

where \mathbf{E}_{dc} is the actual dc electric field. In expressions (8) and (9), the only sum is of course over the Cartesian components. We note that

$$\lim_{\omega \rightarrow 0} \chi^{abc}(-2\omega; \omega, \omega) = \lim_{\omega \rightarrow 0} \chi^{abc}(-\omega; \omega, 0), \quad (10)$$

a statement of the equivalence of the SHG and LEO susceptibilities at zero frequency. This result, which is physically expected and follows from our expression for the susceptibilities (see Appendix A), will be relevant in the context of the discussion of our results.

The χ^{abc} in Eq. (7) can generally be written in the form

$$\begin{aligned} \chi^{abc}(-\omega_\beta - \omega_\gamma; \omega_\beta, \omega_\gamma) &= \chi_{II}^{abc}(-\omega_\beta - \omega_\gamma; \omega_\beta, \omega_\gamma) \\ &+ \eta_{II}^{abc}(-\omega_\beta - \omega_\gamma; \omega_\beta, \omega_\gamma) \\ &+ \frac{i}{(\omega_\beta + \omega_\gamma)} \sigma_{II}^{abc}(-\omega_\beta \\ &- \omega_\gamma; \omega_\beta, \omega_\gamma). \end{aligned} \quad (11)$$

The first term in Eq. (11) represents the purely interband contribution that would result if one thought of the system as only a set of ‘‘effective’’ atoms labeled by their crystal momenta. The second term describes the contribution from the modulation of the linear susceptibility by the intraband motion of the electrons. The third term represents that portion of the susceptibility resulting from the modification of the intraband motion by the polarization energy associated with the interband motion. A more thorough analysis and interpretation of these terms has already been presented.²⁸ The explicit definitions of the terms in Eq. (11) specific to the SHG and LEO susceptibilities are given in Appendix B.

B. “Scissors” approximation and implementation

While the Kohn-Sham equations form a fundamental starting point for the determination of ground-state properties, the unoccupied conduction bands that are calculated have no direct physical significance. Indeed, if they are used naively as single-particle states in a calculation of optical properties for typical semiconductors, the so-called “band-gap” problem results: the absorption starts at much too low an energy.² At a basic level, many-body effects must be included in calculating not only the ground-state properties but the response to an applied perturbation,^{34,35} to do this, the GW approximation for the self-energy operator has been employed by a number of workers.^{36–41} Instead of following this route, we take the simpler approach of Levine and Allan⁶ and introduce a “scissors approximation” to account for the self-energy effects. Although this technique is at best semi-phenomenological, it rests on the fact that GW calculations often indicate little change in the single-electron Green function even with the inclusion of many-body effects; only the energy gap is significantly modified.³⁷ Further, it has been suggested recently that the scissors approximation can find justification⁴² in the necessity of using a polarization-dependent energy functional.⁴³ Whatever the final verdict on that proposal, our view is that the approach constitutes a simple extension of a ground-state calculation that will allow for relatively easy first investigations of linear and nonlinear optical properties; within this spirit it has been used in a number of calculations,^{6,17–19,44,45} although we are among the first to employ it in calculating the optical response over a wide energy range.

A point that requires some degree of care is the appearance of the scissors shift in the expressions for the linear and nonlinear response. Actually, in the length gauge calculation we use here the result is straightforward; but for comparison with other work we briefly outline here the inclusion of the scissors operator, and detail how from different perspectives rather more complicated expressions can result, and have appeared in the literature.^{18,45} In the length gauge, before the scissors operator is included, the Hamiltonian from which the response functions are calculated²⁹ is given by

$$H = \frac{p^2}{2m} + V(\mathbf{r}) - e\mathbf{r} \cdot \mathbf{E}, \quad (12)$$

where $V(\mathbf{r})$ is a periodic potential, \mathbf{r} the position operator, and the electric field is $\mathbf{E} = -\dot{\mathbf{A}}/c$. The simplest and most obvious way to correct for the underestimation of the band gap is to include in this Hamiltonian a \mathbf{k} -independent energy shift “projected” onto the conduction states.⁶ Within this approximation the Hamiltonian takes the form

$$\tilde{H} = H + V_s, \quad (13)$$

with

$$V_s = \Delta \sum_{c\mathbf{k}} |c\mathbf{k}\rangle \langle c\mathbf{k}|, \quad (14)$$

where the sum in V_s is over all \mathbf{k} and conduction bands c ; Δ is the constant energy shift associated with the correction of the band gap; the $|c\mathbf{k}\rangle$ represent single-particle eigenstates of the unperturbed Hamiltonian, $H_0 = p^2/2m + V(\mathbf{r})$.

The effect of the inclusion of the scissors operator within our formalism is to modify the expressions for the response functions in a straightforward way. As an illustration, we consider the linear response coefficient. With \tilde{H} as the governing Hamiltonian, Eq. (4) becomes

$$\tilde{\chi}_I^{ab}(-\omega; \omega) = \frac{e^2}{\Omega \hbar} \sum_{nm\mathbf{k}} f_{nm} \frac{r_{nm}^a(\mathbf{k}) r_{mn}^b(\mathbf{k})}{\omega_{mn}(\mathbf{k}) + (\Delta/\hbar)(\delta_{mc} - \delta_{nc}) - \omega}, \quad (15)$$

where the c in the Kronecker δ 's refers to a conduction state and the tilde indicates that this coefficient is derived from \tilde{H} . The form of this function is essentially identical to the previous expression without the scissors operator. The only change has been the modification of the energy difference,

$$\omega_{mn} \rightarrow \omega_{mn} + \frac{\Delta}{\hbar} (\delta_{mc} - \delta_{nc}). \quad (16)$$

An important point to note is that the matrix elements of the position operator remain unchanged. This follows because implicit in the approximation in Eq. (13) is the assumption that the effective wave functions do not change when many-body effects are included.³⁷ This analysis has been carried out for second-order response with the same result: the new expressions are identical except for the change in the ω_{mn} as described above.

In practice, one does not directly calculate the matrix elements of the position operator \mathbf{r}_{nm} , but rather the velocity matrix elements \mathbf{v}_{nm} . Consequently, a necessary step in the conversion of the response function expressions to numerically amenable form is to make a correspondence between these two different matrix elements. This correspondence is affected by the inclusion of the scissors operator in our Hamiltonian.

We first consider linear response in the absence of the scissors operator. The \mathbf{v}_{nm} are then determined from

$$\mathbf{v} = \frac{1}{i\hbar} [\mathbf{r}, H], \quad (17)$$

with the result of Eq. (5) for the elements of the position operator with $\omega_{nm} \neq 0$. In terms of the $\mathbf{v}_{nm}(\mathbf{k})$, Eq. (4) can be written in the form

$$\chi_I^{ab}(-\omega; \omega) = \frac{e^2}{\Omega \hbar} \sum_{nm\mathbf{k}} f_{nm} \frac{v_{nm}^a(\mathbf{k}) v_{mn}^b(\mathbf{k})}{\omega_{mn}^2[\omega_{mn}(\mathbf{k}) - \omega]}. \quad (18)$$

With the scissors operator included in the Hamiltonian, the velocity operator changes. The equation for the modified velocity becomes

$$\tilde{\mathbf{v}} = \frac{1}{i\hbar} [\mathbf{r}, \tilde{H}] = \frac{1}{i\hbar} \{[\mathbf{r}, H] + [\mathbf{r}, V_s]\}, \quad (19)$$

from which we obtain the analog of Eq. (5):

$$\mathbf{r}_{nm} = \frac{\tilde{\mathbf{v}}_{nm}}{i[\omega_{nm} + (\Delta/\hbar)(\delta_{nc} - \delta_{mc})]}. \quad (20)$$

Since the \mathbf{r}_{nm} do not change when the scissors operator (14) is included we can determine the relationship between the velocity matrix elements with the scissors operator, and those without. We find

$$\tilde{\mathbf{v}}_{nm} = \mathbf{v}_{nm} \frac{\omega_{nm} + (\Delta/\hbar)(\delta_{nc} - \delta_{mc})}{\omega_{nm}}. \quad (21)$$

It is now possible to write the linear response coefficient within the scissors approximation in terms of the velocity matrix elements, as was done in Eq. (18). We use the correspondence of Eq. (20) to write

$$\begin{aligned} \tilde{\chi}_I^{ab}(-\omega; \omega) &= \frac{e^2}{\Omega \hbar} \sum_{nmk} f_{nm} \frac{\tilde{v}_{nm}^a(\mathbf{k}) \tilde{v}_{mn}^b(\mathbf{k})}{[\omega_{mn}(\mathbf{k}) + (\Delta/\hbar)(\delta_{mc} - \delta_{nc}) - \omega]} \\ &\times \frac{1}{[\omega_{mn} + (\Delta/\hbar)(\delta_{mc} - \delta_{nc})]^2}. \end{aligned} \quad (22)$$

Yet, in order to actually calculate this coefficient we need to have it expressed in terms of the unmodified velocity matrix elements, the matrix elements we obtain from the LDA calculation. To do this we use Eq. (21) and write Eq. (22) as

$$\begin{aligned} \tilde{\chi}_I^{ab}(-\omega; \omega) &= \frac{e^2}{\Omega \hbar} \sum_{nmk} f_{nm} \frac{v_{nm}^a(\mathbf{k}) v_{mn}^b(\mathbf{k})}{\omega_{mn}^2 [\omega_{mn}(\mathbf{k}) + (\Delta/\hbar)(\delta_{mc} - \delta_{nc}) - \omega]}. \end{aligned} \quad (23)$$

As can be seen from the above equation, the linear response function within the scissors approximation is no more computationally difficult to calculate than that without the scissors approximation [Eq. (18)]. Note that Eqs. (15), (22), and (23) are all equivalent, and that Eq. (23) follows directly from Eq. (15) by the use of Eq. (5). Furthermore, the approach taken in deriving Eq. (23) is easily extended to higher-order response functions; we find that, as for linear response, the extension of a response coefficient expression to the scissors approximation consists of two steps: First the function, written using the matrix elements of the position operator, is modified as indicated by Eq. (16). Second, we need only use Eq. (5) to write the response function in terms of $\mathbf{v}_{nm}(\mathbf{k})$, producing the analog of Eq. (23), to make it suitable for numerical evaluation.

We note that the result in Eq. (23) is essentially equivalent to that introduced by Del Sole and Girlanda,⁹ and Levine and Allan.^{6,18,44} However, Del Sole and Girlanda restrict their discussion to linear response, where we have extended this approach to any higher-order response function. Levine and Allan do treat second-order susceptibilities within the scissors approximation but do so in a way specific to their formalism for nonlinear response. Our approach for the scissors operator, although equivalent, is a general extension of this previous work applied to our formalism.

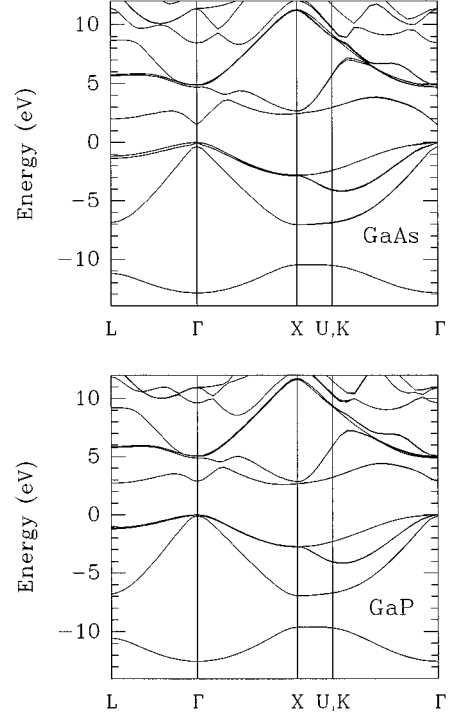


FIG. 1. FLAPW electronic band structures for GaAs and GaP. The fundamental band gap has been adjusted within the scissors approximation.

III. METHOD OF CALCULATION

A. FLAPW method

In order to determine the optical response functions in a full band structure approach, one requires the eigenvalues and velocity matrix elements at many \mathbf{k} points in the Brillouin zone (BZ). The velocity matrix elements, in turn, require a knowledge of the electronic wave functions. For this purpose, we employ a first-principles approach in the form of the FLAPW method. As this method has been previously discussed,^{31,32} we highlight only a few of its pertinent features.

The spirit of the FLAPW approach is the partitioning of real space within a crystal into two distinct regions: “muffin-tin” spheres surrounding the atomic positions, and the remaining interstitial space. The electronic wave functions then have a dual representation over all space, consisting of an expansion of solutions of the Schrödinger equation and its energy derivative in the muffin-tin spheres, and plane waves in the interstitial region. We rely on the LDA for the one-electron exchange-correlation potential. Prior to determining the electronic structure and wave functions at \mathbf{k} points of interest in the BZ, we converge the charge density in the crystal in a series of self-consistent calculations. This convergence process involves all electrons, and so the valence and core electronic states are recalculated for each iteration.

In the calculation of the electronic band structure of GaAs and GaP we have used the Wigner interpolation method as a means of determining the one-electron exchange-correlation potential. Spin-orbit and scalar relativistic effects are included in both calculations. We present in Fig. 1 the band structures for GaAs and GaP. In both band structures we

have adjusted the band gap to agree with experiment using the scissors approximation, as discussed in the previous section.

B. Response functions

The evaluation of each of the response functions is carried out in a slightly different way, but there are some general considerations that need to be addressed in all cases. One necessary step in evaluating optical response is the reduction of the analytic expressions for the susceptibilities to ones suitable for computation. The details of this procedure for each of the response functions are too long to present here, but we will outline the general approach.

The expressions for the susceptibilities are first written in terms of the velocity matrix elements rather than the matrix elements of the position operator and converted to an integral over the BZ rather than a sum over \mathbf{k} . If the response function is sought above the band gap, the imaginary part is extracted, for which there is a δ function present in the integrand; in the case of cubic symmetry some further simplifications can be made to the second-order susceptibilities.

For linear response we evaluate the imaginary part of the dielectric function given in Eq. (6), which is already in a form amenable to computation. We obtain the real part of the dielectric function by using the Kramers-Kronig relation. The SHG response function, as given in Appendix B, requires some manipulation prior to being calculated. Again, since we seek the response above and below the band gap, we evaluate the imaginary part and obtain the real part from the Kramers-Kronig relation for this function.⁴⁶ The LEO susceptibility is evaluated below the band gap only, where it is of primary interest, and so we calculate it directly in this energy regime.

We use the symmetry of the crystal to reduce the integration over the BZ to one over the irreducible segment of the BZ (IBZ). This is done by applying the operators P_R of the group elements R of the symmetry group T_d (applicable for the semiconductors considered here), to the expansion dyadics of the response tensor. For linear response, we consider the dielectric tensor

$$\vec{\epsilon}_2(\omega) = \sum_{ab} \hat{a}\hat{b}\epsilon_2^{ab}, \quad (24)$$

and after applying the operators P_R we obtain

$$\begin{aligned} \sum_R P_R(\hat{x}\hat{x}) &= \sum_R P_R(\hat{y}\hat{y}) = \sum_R P_R(\hat{z}\hat{z}) = 8\vec{\mathbb{1}}, \\ \sum_R P_R(\hat{a}\hat{b}) &= 0, \quad i \neq j, \end{aligned} \quad (25)$$

where $\vec{\mathbb{1}}$ is the identity tensor. Thus only the diagonal element survives, as is well known. With the use of these symmetry elements and the inversion symmetry of the BZ, the integration over \mathbf{k} can be restricted to the IBZ only.

For second-order optical response we proceed in the same way. We write the SHG susceptibility as

$$\vec{\chi}(-2\omega; \omega, \omega) = \sum_{abc} \hat{a}\hat{b}\hat{c}\chi^{abc}(-2\omega; \omega, \omega), \quad (26)$$

and applying the operators P_R we find

$$\sum_R P_R(\hat{x}\hat{y}\hat{z}) = 4(\hat{x}\hat{y}\hat{z} + \hat{y}\hat{x}\hat{z} + \hat{x}\hat{z}\hat{y} + \hat{y}\hat{z}\hat{x} + \hat{z}\hat{x}\hat{y} + \hat{z}\hat{y}\hat{x}),$$

$$\sum_R P_R(\hat{a}\hat{b}\hat{c}) = 0, \quad a, b, c \text{ not all different.} \quad (27)$$

It can be seen from Eq. (27) that there is only one independent component for the SHG susceptibility that we take to be χ^{xyz} ; the same result follows for the LEO susceptibility.

In the evaluation of all the response functions, the essential task becomes the integration of a function over the IBZ. This we do in a ‘‘hybrid’’ random sampling-tetrahedron method. We partition the IBZ into many small tetrahedra, at whose vertices we evaluate the eigenvalues and velocity matrix elements based on results from the FLAPW calculations. We then ‘‘linearize’’ the energy differences ω_{nm} as well as the matrix element product in the integrand of the response function. Although it has been suggested that the matrix elements can be taken to be constant over a tetrahedron,⁴⁷ we feel that the validity of this approximation becomes increasingly questionable in the complicated products of these matrix elements found in the higher-order susceptibilities. Having linearized these quantities over a tetrahedron, we then sample a large number of randomly chosen points within a given tetrahedron and at each evaluate the integrand. This approach has the advantage of being much easier to implement than the linear-analytic tetrahedron method,⁴⁸ which becomes complicated for nonlinear response functions.⁴⁹

In the calculation of all the susceptibilities, we directly evaluate the velocity matrix elements and eigenvalues from the FLAPW calculation at 1365 \mathbf{k} points in the IBZ; this corresponds to the partitioning of this region into 5184 tetrahedra. We have further partitioned the region around the Γ point into 3993 smaller tetrahedra, which requires the matrix elements and eigenvalues at 1092 \mathbf{k} points. The reason for this finer mesh of points near the Γ point is that we have found that there is some sensitivity in the nonlinear response functions to numerical approximations in this region.^{19,24} The susceptibilities calculated from this number of \mathbf{k} points are only marginally different from a calculation involving only half this number. On this basis, it is clear that our current calculation should suffer only a limited numerical error using this particular integration scheme.

IV. RESULTS AND DISCUSSION

In Fig. 2 we present our results for the imaginary part of the dielectric function, $\epsilon_2(\omega)$, for GaAs and GaP. The experimental results of Philipp and Ehrenreich,⁵⁰ and Aspnes and Studna⁵¹ are included for comparison. The main features of the linear response function can be attributed to the same regions of the electronic band structure for both materials. These features are largely governed by the joint density of states, whose structure is associated with those regions in the band structure for which pairs of bands are essentially parallel. In particular, using the terminology specific to zincblende semiconductors,⁵² we can identify the dual peak structure at low energy with the E_1 and $E_1 + \Delta_1$ transitions. The main peak and the slight shoulder to the left of this peak

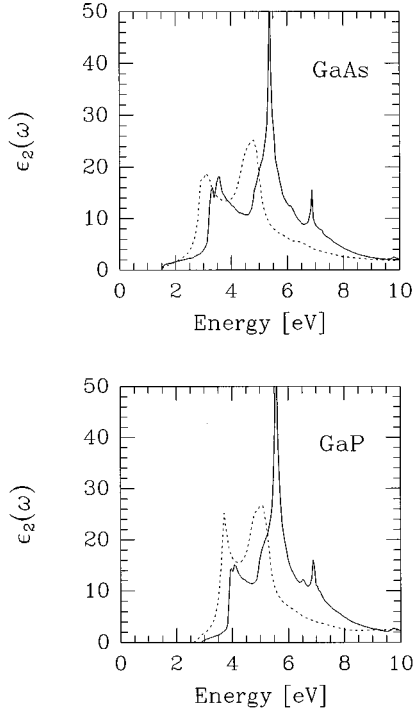


FIG. 2. Results for the calculated imaginary part of the dielectric function, $\epsilon_2(\omega)$ (solid line), for GaAs and GaP. Energy bin size is 0.05 eV. Experimental results (dotted line) are from Philipp and Ehrenreich (Ref. 50), and Aspnes and Studna (Ref. 51).

are due to the E_2 and E'_0 transitions, respectively. Finally, the high-energy feature in the spectrum is attributed to the E'_1 optical transition.

It is evident from Fig. 2 that our calculation predicts the peak positions higher in energy than those in the experimental results. All *ab initio* calculations share a difficulty in correctly predicting both the band gap and the peak positions in the linear response spectrum. The original first-principles work of Wang and Klein² employed the LDA and achieved some agreement in peak positions, but underestimated the fundamental band gap. A rigid adjustment of the electronic structure calculated by Wang and Klein, following the scissors approximation adopted here, would result in a similar mispositioning of the location of the peaks in the linear response function. The more recent work of Huang and Ching^{21,20} using the orthogonalized linear combination of atomic orbitals method for the electronic structure calculation and a scissors correction, has obtained only limited agreement with experiment for the dispersion of the dielectric function. Alouani, Brey, and Christensen⁵ have achieved some success lately in calculating linear response for GaAs, accurately predicting both the band gap and the dispersion in $\epsilon_2(\omega)$. Their method involves adding in sharply peaked potentials within their LDA framework in such a way that the low band gap is suitably “compensated.” Although arguably no more phenomenological than the simple scissors approximation we employ here, its ultimate justification and extension to a more fundamental level is perhaps less clear.

We make two further comments concerning $\epsilon_2(\omega)$: First, the intensity of the peaks in the calculated function is overestimated in part due to the exclusion of the effects of a finite relaxation time. Second, the experimental results in Fig. 2

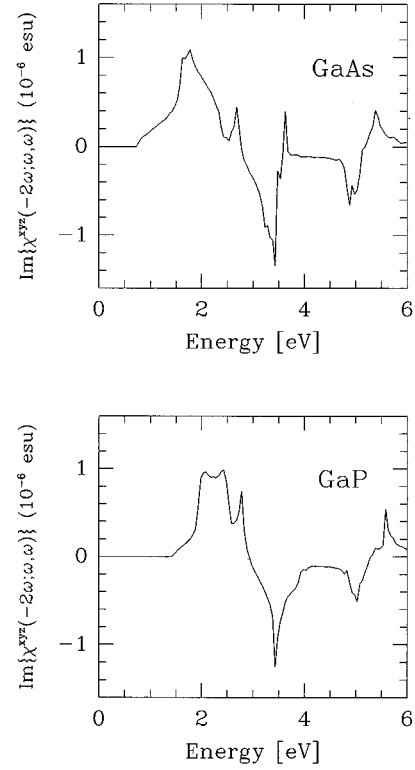


FIG. 3. Plot of $\text{Im}\{\chi^{xyz}(-2\omega; \omega, \omega)\}$ for GaAs and GaP. The energy bin size is 0.05 eV.

are taken at room temperature; experimental work suggests that peak positions shift to higher energy at lower temperatures.⁵³ A shift of approximately 0.1 eV could be expected for equivalent results at low temperature, which would be more appropriate for comparison with this zero-temperature theoretical work. Yet it is clear that the \mathbf{k} -independent rigid shift in the conduction states with the corresponding modification of the response function expression achieves only reasonable accuracy in the dispersion of the dielectric function.

We note that there has been some recent success at the level of linear response in work based on quasiparticle calculations that treat the self-energy corrections more carefully.⁷ As our emphasis is on the nonlinear optical response, we feel that the scissors approach is an appropriate compromise between computationally amenable calculations and accurate results.

The results for the imaginary part of the SHG susceptibility, $\text{Im}\{\chi^{xyz}(-2\omega; \omega, \omega)\}$, are plotted in Fig. 3. Although this part of the response function cannot be directly compared with experiment, it can be more meaningfully related to the band structure than can $|\chi^{xyz}(-2\omega; \omega, \omega)|$, to which experiments are more directly sensitive. The structure in $\text{Im}\{\chi^{xyz}(-2\omega; \omega, \omega)\}$ can be attributed to the same general regions in the band structure for both GaAs and GaP. The onset of the function occurs at the 2ω resonance with the E_0 optical transition. The first peak is associated with the 2ω resonance with the E_1 and $E_1 + \Delta_1$ optical transitions. The second structure in the function for the most part arises from the 2ω resonance with E'_0 . The complicated structure in the region between 3 and 4 eV is associated with an in-

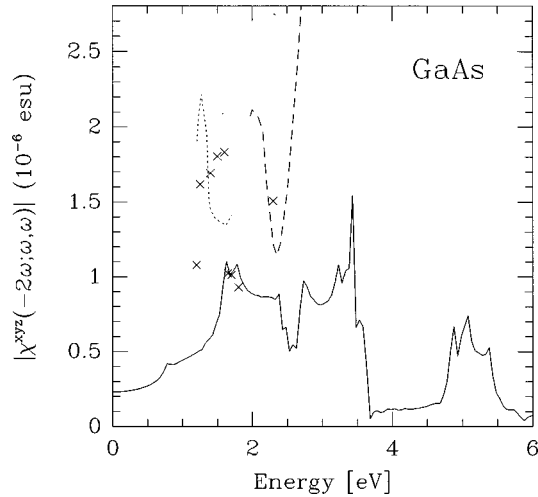


FIG. 4. Absolute value of the SHG susceptibility, $|\chi^{xyz}(-2\omega; \omega, \omega)|$ (solid line), for GaAs. Experimental results are as follows: Parsons and Chang (Ref. 62) (dotted line); Bethune, Schmidt, and Shen (Ref. 63) (dashed line), and Chang, Ducuing, and Bloembergen (Ref. 64) (crosses).

terference between an ω resonance with the E_1 transition and a 2ω resonance with the E_2 and E_1' transitions, while the structure between 5.0 and 5.5 eV is due mainly to the ω resonance with the E_2 optical peak.

Our results for the imaginary part of the SHG susceptibility show important differences from those of Huang and Ching,^{20,21} although there are some similarities in the shapes of the calculated functions. It is important to note that their failure to adjust the velocity matrix elements after rigidly shifting the conduction states to higher energy can result in an appreciable error in their reported values. Levine has suggested that their results could be underestimated by up to a factor of two;¹⁸ this has been corroborated by our own investigations, comparing calculations with and without the matrix elements appropriately modified. The results of Ghahramani *et al.*^{26,54} are closer to ours, despite the differences in approach to the calculation of the electronic band structure. They employ a semi-*ab initio* minimal-basis linear combination of Gaussian orbitals (MLCGO) method.

The absolute value of the SHG susceptibility is plotted in Fig. 4 for GaAs and Fig. 5 for GaP. Experimental data at energies above the gap are very scarce for the materials considered here. The only data we are aware of are for GaAs, and these are plotted in Fig. 4. The experimental results seem largely contradictory and any serious comparison would remain inconclusive.

There is a considerable amount of data available for the LEO susceptibility and, as the chief interest is in the region below the band gap, we have concentrated our investigation to this regime. Two main issues must be addressed, however, in order to make a suitable comparison of our results to the experimental data. The first is that we require an expression that relates the experimentally measured LEO coefficient $r^{xyz}(\omega)$ to our calculated LEO susceptibility $\chi^{xyz}(-\omega; \omega, 0)$; although straightforward, to avoid confusion this is presented in Appendix C. A second issue in the comparison to experiment is that our calculated quantity is in fact the electronic or “clamped” LEO susceptibility. Some of the

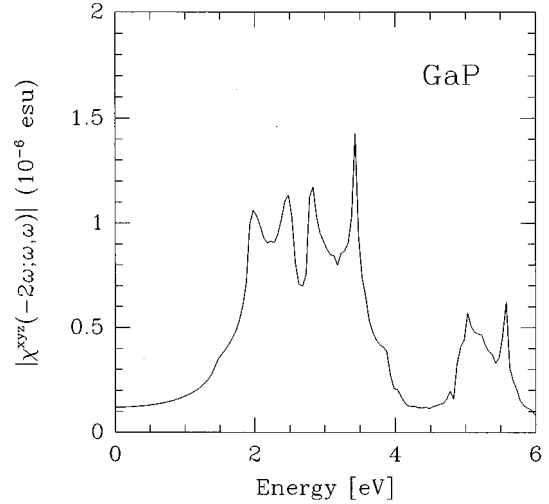


FIG. 5. Absolute value of the SHG susceptibility, $|\chi^{xyz}(-2\omega; \omega, \omega)|$ (solid line), for GaP.

experimental data are in terms of the unclamped values and so must be modified to yield the corresponding clamped LEO coefficient values. To do this we use the compilation of experimental coefficients presented by Adachi,⁵² where estimates of the clamped values are given for those experiments that determined only the unclamped values.

In Fig. 6 and Fig. 7 we plot $\chi^{xyz}(-\omega; \omega, 0)$ for GaAs and GaP in pm/V, as this is the more commonly quoted unit in the literature. We have also plotted $|\chi^{xyz}(-2\omega; \omega, \omega)|$ on the same graph, for a purpose discussed below. The experimental data are presented for comparison. To generate the experimental $\chi^{xyz}(-\omega; \omega, 0)$ we have used Eq. (C8) with the experimentally measured LEO coefficient $r^{abc}(\omega)$ and the index of refraction from Palik.^{55,56}

The results of our calculation are in good agreement with experiment over a large range of frequencies. This agreement is somewhat better for GaAs than for GaP, but given the

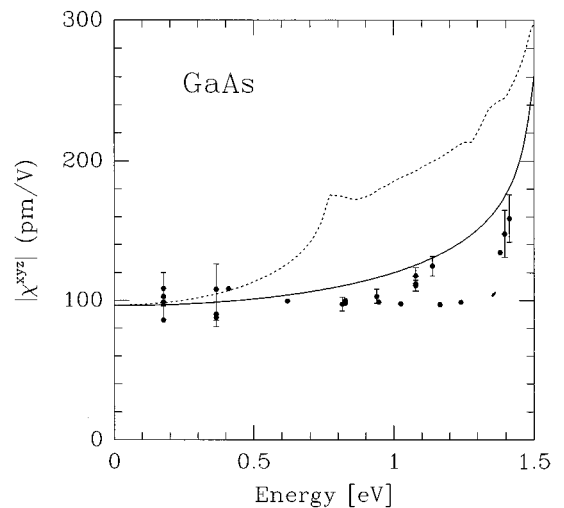


FIG. 6. Plot of second-order optical response in GaAs below the fundamental band gap: LEO susceptibility $\chi^{xyz}(-\omega; \omega, 0)$ (solid line) and the absolute value of the SHG susceptibility $|\chi^{xyz}(-2\omega; \omega, \omega)|$ (dotted line). Experimental results for the LEO effect (solid circles) are from 65–75 as compiled by Adachi (Ref. 52).

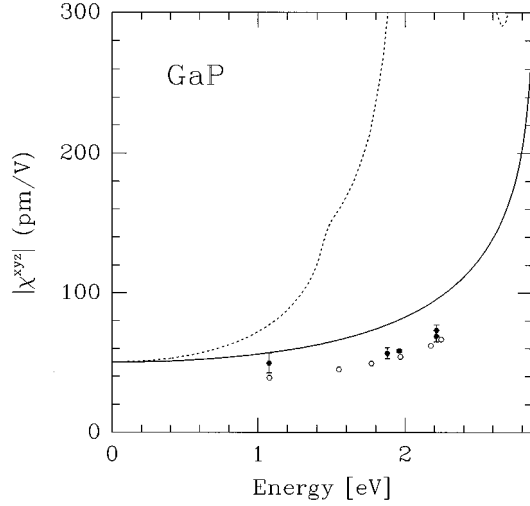


FIG. 7. Plot of second-order optical response in GaP below the fundamental band gap: LEO susceptibility $\chi^{xyz}(-\omega; \omega, 0)$ (solid line) and the absolute value of the SHG susceptibility $|\chi^{xyz}(-2\omega; \omega, \omega)|$ (dotted line). Experimental results for the LEO effect are from Nelson and Turner (Ref. 76) (open circles) and Berozashvili *et al.* (Ref. 77) (solid circles).

complexity of this calculation we feel it is nonetheless quite satisfactory. As we have previously discussed, our calculation is based on a formalism that is well behaved at low frequencies, so the results are believable in the energy regime presented in Figs. 6 and 7. To our knowledge this is the first *ab initio* calculation of the LEO susceptibility for GaAs and GaP. Ghahramani and Sipe have presented the LEO susceptibility for GaAs based on a semiempirical MLCGO calculation,⁵⁷ employing the same nonlinear response formalism given here. Our results are close to this previous work, although we obtain better general agreement with the experimental data for all energies. Various other theoretical calculations of the LEO coefficient have been presented, but these are phenomenological in nature and will not be discussed here.^{10–12}

As there is considerable interest in the optical response at low frequencies, we have presented in Table I our results for the dielectric constant, the SHG susceptibility, and the LEO (clamped lattice) susceptibility for GaAs and GaP at zero-frequency. We have included for comparison other theoretical calculations, and experimental results. For linear response our agreement with experiment is excellent for both materials. We recognize that this may be somewhat fortuitous, given the comparison of our results with experiment over a broad frequency range. A shift of our calculated peaks in $\epsilon_2(\omega)$ to lower energies, towards the experimental peaks, would result in a higher calculated $\epsilon(0)$; this would be partly offset by the inclusion of local field effects, which have been shown to reduce the zero-frequency result for the materials considered here.¹⁸

The results for $\chi^{xyz}(0)$ require more discussion, in light of the wide range of values that appears. We first recall, as noted in Sec. II [see Eq. (10)] that the SHG and LEO (clamped lattice) susceptibilities are equal at zero frequency. This is not only a numerical result of the present calculation: We have shown this analytically within our formalism, and in any case it would be expected on physical grounds. Yet

TABLE I. The linear and second order optical response in GaAs and GaP at zero frequency. The results of the present calculation (FLAPW) are compared with other theoretical calculations and experimental data.

Material	Method	$\epsilon(0)$	$\chi^{xyz}(0)$ (pm/V)	
			SHG	LEO
GaAs	FLAPW	10.9	96.5	96.5
	Pseudopotential ^a	11.0	172	
	OLCAO ^b	11.21	251.3	
	MLCGO		104.3 ^c	104.3 ^d
	Experiment	10.9 ^e	162 ± 10 ^f	99.8 ^g
GaP	FLAPW	9.0	50.3	50.3
	Pseudopotential ^a	8.8	75	
	OLCAO ^b	9.29	134.9	
	MLCGO		43.6 ^c	
	Experiment	9.1 ^h	74 ± 4 ^f	44.3 ⁱ

^aLevine and Allan (Ref. 19).

^bHuang and Ching (Ref. 21).

^cGhahramani *et al.* (Refs. 26 and 54).

^dGhahramani and Sipe (Ref. 57).

^eReference 55.

^fLevine and Bethea (Ref. 59) value at 0.117 eV, as revised by Roberts (Ref. 58).

^gAverage of experimental values at 0.117 eV, from Adachi (Ref. 52).

^hReference 56.

ⁱAverage of experimental values at 1.08 eV, from Adachi (Ref. 52).

there is significant disagreement between the experimental results for the zero-frequency SHG and LEO susceptibilities. This disagreement does not seem to have been fully appreciated.

Our calculated results are in closest agreement with the MLCGO calculation of Ghahramani *et al.*^{26,54} We note that their calculation and ours are completely independent and are based on markedly different approaches to the determination of the electronic structure and the velocity matrix elements. The orthogonalized LCAO calculation of Huang and Ching²¹ leads to a much higher result for $\chi^{xyz}(0)$ than the present work. And, as we have previously discussed, we believe that they require an adjustment of their velocity matrix elements in accordance with their scissors shift. With such an adjustment their value for $\chi^{xyz}(0)$ would be raised even higher, exceedingly high in comparison with other theoretical calculations and with experimental values. Levine has presented the most comprehensive work below band-gap energies of which we are aware.¹⁹ But his formulation of the SHG susceptibility is drastically different from that used here, and thus it is unfortunately difficult to identify the reasons for the disparity between the results.

Yet we note that our calculated results are in extremely good agreement with the LEO experimental results. Given that various LEO experiments done recently seem to corroborate each other, we would suggest that this gives strong support to the value of $\chi^{xyz}(0)$ we have calculated here. As to its disagreement with the SHG experimental results, we note that the values given in Table I are from Roberts,⁵⁸ who revised the original values of Levine and Bethea.⁵⁹ Their

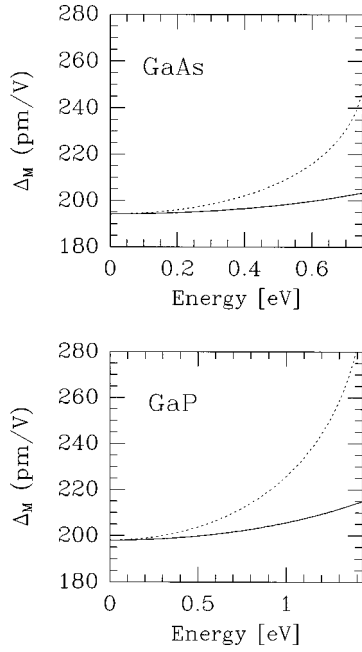


FIG. 8. Plot of Miller's Δ_M below half the band gap for GaAs and GaP: Δ_M^{SHG} (dotted line) and Δ_M^{LEO} (solid line).

experiments were conducted more than two decades ago, and it is not clear these data should be given as much weight as the much more recent and consistent work on the LEO susceptibilities in attempting to establish an experimentally determined value of $\chi^{xyz}(0)$. Certainly the discrepancy between the experimental results for the two equivalent susceptibilities indicates that more recent experimental studies would be helpful in resolving this issue.

It is interesting in the context of the current calculation to assess the validity of ‘‘Miller's rule’’ based on our theoretical results. Miller proposed that the quantity

$$\Delta_M(\omega_1 + \omega_2) = \frac{\chi^{(2)}(-\omega_1 - \omega_2; \omega_1, \omega_2)}{\chi^{(1)}(\omega_1 + \omega_2)\chi^{(1)}(\omega_1)\chi^{(1)}(\omega_2)} \quad (28)$$

is approximately constant for a wide range of noncentrosymmetric materials, with little variation in frequency.⁶⁰ As we have calculated two second-order susceptibilities we can investigate Miller's Δ_M in both cases. We have for SHG,

$$\Delta_M^{\text{SHG}}(2\omega) = \frac{\chi^{xyz}(-2\omega; \omega, \omega)}{\chi^{(1)}(2\omega)[\chi^{(1)}(\omega)]^2}, \quad (29)$$

a form specific to the zinc-blende materials considered here, given that there is only one independent component for the SHG susceptibility and equal diagonal components for $\chi^{(1)}$. For the LEO effect, the corresponding quantity is

$$\Delta_M^{\text{LEO}}(\omega) = \frac{\chi^{xyz}(-\omega; \omega, 0)}{[\chi^{(1)}(\omega)]^2\chi^{(1)}(0)}. \quad (30)$$

We plot in Fig. 8 both of these functions for GaAs and GaP. Several comments can be made about our results for Miller's Δ_M . First we note that Δ_M^{SHG} is equal to Δ_M^{LEO} at zero frequency. We would expect this result given the equivalence of Eqs. (29) and (30) at zero frequency if the second-order susceptibilities are equivalent in this limit as

well. As can be seen in Fig. 8 there is a definite variation in frequency for both Δ_M^{SHG} and Δ_M^{LEO} . Both functions show an increase with increasing frequency, although Δ_M^{LEO} rises less rapidly than Δ_M^{SHG} . The zero-frequency value of Δ_M for both materials is remarkably similar; this corroborates Miller's original conjecture, but it is clear that an analysis of a wider range of materials would be necessary to test this further.

We note that our theoretical results for Δ_M^{SHG} are very similar to that of Levine.¹⁹ The magnitudes are somewhat different, due to the differences in our $\chi^{xyz}(-2\omega; \omega, \omega)$ results compared with theirs, but the trend in Δ_M^{SHG} is the same. Huang and Ching's²¹ results for Δ_M^{SHG} seems somewhat anomalous; they predict Δ_M^{SHG} to be a flat or slightly decreasing function over the energy range plotted in Fig. 8.

V. CONCLUSIONS

We have presented results for linear and second-order optical response in GaAs and GaP based on a first-principles FLAPW electronic structure calculation. We have employed a response formalism that is free of any unphysical divergences at zero frequency, providing believable results across the entire energy spectrum for any response function. Within this formalism we have implemented the scissors approximation, and have fully accounted for the modification of the velocity matrix elements that appear more explicitly in other calculation schemes. The response function expressions within the scissors approximation are straightforward to obtain, and are no less amenable to computation than without the scissors correction.

Our results for the imaginary part of the dielectric function $\epsilon_2(\omega)$ show only reasonable agreement with experiment across a broad energy range, although we obtain excellent agreement with experiment for $\epsilon(0)$. This illustrates the possible limitations of the scissors approximation and indicates that good zero-frequency results do not necessarily imply a good prediction of the dispersion of the dielectric function.

The SHG susceptibility has been presented and it shows important differences from other theoretical calculations. The lack of experimental data, as well as its contradictory nature, prevents any conclusive comparison with experiment over a large energy range. A comparison of zero-frequency results for the SHG susceptibility shows that our calculation is closest to Ghahramani *et al.*,^{26,54} but there is large disparity between existing theoretical calculations and experimental data.

We have also calculated the LEO susceptibility below the band gap, and here our results are in excellent agreement with experiment throughout the experimentally studied energy regime. Since the SHG and LEO (clamped lattice) susceptibilities are equal at zero frequency, the more recent work on the LEO susceptibility (with which our calculations are in excellent agreement) is thus in contradiction with the much older work on the SHG susceptibility (with which our calculations are in disagreement). This both gives us confidence in our calculated results, and—whatever the status of our calculation—encourages us to urge our experimental colleagues to reinvestigate the SHG susceptibility both at low frequency and over a wide frequency range.

ACKNOWLEDGMENTS

The authors are very grateful to Professor Henry Krakauer of the College of William and Mary for providing us with the FLAPW program, as well as for helpful discussions on making LDA calculations. We also acknowledge useful discussions with Dr. Claudio Aversa of the University of California at Santa Barbara. This work was supported by the Natural Sciences and Engineering Research Council of Canada and the Ontario Laser and Lightwave Research Centre.

APPENDIX A: SUSCEPTIBILITY CONVENTIONS

In this appendix we establish our convention for the optical susceptibilities and the definition of frequency components, and for clarity mention other conventions in common use and how the resulting expressions differ from ours. In Appendix C we detail the connection between $\chi^{abc}(-\omega; \omega, 0)$ and the usual electro-optic coefficient $r^{abc}(\omega)$. On these matters various usages exist in the literature, often never explicitly defined. We endeavor here to make our usage, and the way we interpret the quoted experimental results, as clear as possible.

It is useful to identify three conventions that can be used to introduce the frequency components of the fields. In the first,

$$\mathbf{E}(t) = \sum_{\omega_i \geq 0} \text{Re}[\mathbf{E}(\omega_i) e^{-i\omega_i t}] = \frac{1}{2} \sum_{\omega_i \neq 0} \mathbf{E}(\omega_i) e^{-i\omega_i t} + \mathbf{E}(0), \quad (\text{A1})$$

where in the second expression generally $\mathbf{E}(-\omega_i) \equiv \mathbf{E}^*(\omega_i)$, and thus $\mathbf{E}(0)$ is taken to be real. Clearly in this first convention the actual dc field, \mathbf{E}_{dc} , is just $\mathbf{E}_{\text{dc}} = \mathbf{E}(0)$. The second convention corresponds to introducing $\mathbf{E}(\omega_i)$, which are half those appearing in the first convention; here the same electric field $\mathbf{E}(t)$ is written as

$$\mathbf{E}(t) = 2 \sum_{\omega_i \geq 0} \text{Re}[\mathbf{E}(\omega_i) e^{-i\omega_i t}] = \sum_{\omega_i \neq 0} \mathbf{E}(\omega_i) e^{-i\omega_i t} + 2\mathbf{E}(0). \quad (\text{A2})$$

In this convention the actual dc field is given by $\mathbf{E}_{\text{dc}} = 2\mathbf{E}(0)$. Finally, one can adopt a third convention that differs from the second only by the treatment of the field component at zero frequency:

$$\mathbf{E}(t) = \sum_{\omega_i \neq 0} \mathbf{E}(\omega_i) e^{-i\omega_i t} + \mathbf{E}(0) = \sum_{\omega_i} \mathbf{E}(\omega_i) e^{-i\omega_i t}. \quad (\text{A3})$$

Here $\mathbf{E}_{\text{dc}} = \mathbf{E}(0)$. We refer to the conventions identified by Eqs. (A1)–(A3), and the corresponding expressions for $\mathbf{P}(t)$, as conventions (1)–(3), respectively.

In all conventions the linear response is specified by

$$P^a(\omega) = \chi_I^{ab}(-\omega; \omega) E^b(\omega), \quad (\text{A4})$$

where superscripts indicate Cartesian components and are to be summed over if repeated. For nonlinear response we restrict ourselves for the moment to convention (2); we generally follow the susceptibility notation of Boyd,³³ adopting,

however, a more common manner of indicating the frequency sum. That is, a nonlinear polarization component is related to the electric field by

$$P^a(\omega_\beta + \omega_\gamma) = \chi^{abc}(-\omega_\beta - \omega_\gamma; \omega_\beta, \omega_\gamma) E^b(\omega_\beta) E^c(\omega_\gamma), \quad (\text{A5})$$

where χ^{abc} indicates the second-order susceptibility. Cartesian components are again summed over if repeated, as are frequency components ω_β and ω_γ , but only such that the sum $(\omega_\beta + \omega_\gamma)$ is held fixed; the susceptibilities are taken to satisfy intrinsic permutation symmetry, $\chi^{abc}(-\omega_\beta - \omega_\gamma; \omega_\beta, \omega_\gamma) = \chi^{acb}(-\omega_\beta - \omega_\gamma; \omega_\gamma, \omega_\beta)$. We derive our perturbation expressions for $\chi^{abc}(-\omega_\beta - \omega_\gamma; \omega_\gamma, \omega_\beta)$ within convention (2), but with all frequency components assumed nonzero; in this case conventions (2) and (3) are identical. A susceptibility involving a zero-frequency component, such as $\chi^{abc}(-\omega; \omega, 0)$, is then obtained from, for example,

$$\chi^{abc}(-\omega; \omega, 0) \equiv \lim_{\omega_0 \rightarrow 0} \chi^{abc}(-\omega - \omega_0; \omega, \omega_0). \quad (\text{A6})$$

Because of the way the frequency components enter the expression (A2) for $\mathbf{E}(t)$ in convention (2), we would physically expect, for example, that

$$\lim_{\omega \rightarrow 0} \chi^{abc}(-2\omega; \omega, \omega) = \lim_{\omega \rightarrow 0} \chi^{abc}(-\omega; \omega, 0), \quad (\text{A7})$$

and this is indeed found.

Turning now to expressions for the polarization in different nonlinear processes, in convention (2) we have, from Eq. (A5),

$$\begin{aligned} P^a(2\omega) &= \chi^{abc}(-2\omega; \omega, \omega) E^b(\omega) E^c(\omega), \\ P^a(\omega + \omega_0) &= 2\chi^{abc}(-\omega - \omega_0; \omega, \omega_0) E^b(\omega) E^c(\omega_0), \\ P^a(\omega) &= 4\chi^{abc}(-\omega; \omega, 0) E^b(\omega) E^c(0), \end{aligned} \quad (\text{A8})$$

for second-harmonic generation, frequency mixing (ω with ω_0), and the linear electro-optic effect, respectively. Here, and in such expressions below, only the Cartesian components are summed over if repeated. Note that the expressions we derive for χ^{abc} can be used within convention (1) by simply replacing in Eq. (A8) $\mathbf{E}(\omega_i)$ by $\mathbf{E}(\omega_i)/2$, and $\mathbf{P}(\omega_i)$ by $\mathbf{P}(\omega_i)/2$. The effect is for the prefactors (1,2,4) appearing respectively in Eq. (A8) to go over to $(\frac{1}{2}, 1, 2)$, the usual prefactors introduced in convention (1). Within convention (3) we have, instead of Eq. (A8),

$$\begin{aligned} P^a(2\omega) &= \chi^{abc}(-2\omega; \omega, \omega) E^b(\omega) E^c(\omega), \\ P^a(\omega + \omega_0) &= 2\chi^{abc}(-\omega - \omega_0; \omega, \omega_0) E^b(\omega) E^c(\omega_0), \\ P^a(\omega) &= 2\chi^{abc}(-\omega; \omega, 0) E^b(\omega) E^c(0). \end{aligned} \quad (\text{A9})$$

However, note that within either convention (2) or (3) we may write

$$\begin{aligned} P^a(2\omega) &= \chi^{abc}(-2\omega; \omega, \omega) E^b(\omega) E^c(\omega), \\ P^a(\omega + \omega_0) &= 2\chi^{abc}(-\omega - \omega_0; \omega, \omega_0) E^b(\omega) E^c(\omega_0), \\ P^a(\omega) &= 2\chi^{abc}(-\omega; \omega, 0) E^b(\omega) E^c_{\text{dc}}. \end{aligned} \quad (\text{A10})$$

That is, when the polarization is written in terms of the actual dc field \mathbf{E}_{dc} the prefactor for the electro-optic effect is the same as the prefactor for frequency mixing. While it is often $\chi^{abc}(-\omega - \omega_0; \omega, \omega_0)$ that is essentially measured, it is the $\omega_0 \rightarrow 0$ limit of this expression, $\chi^{abc}(-\omega; \omega, 0)$, that we calculate, with lattice coordinates fixed. For $\hbar\omega_0$ much less than the electronic energy scales but much larger than phonon energies, these quantities can be expected to be essentially identical. Most often quoted is an experimental result for the electro-optic coefficient $r^{abc}(\omega)$; in Appendix C we relate $\chi^{abc}(-\omega; \omega, 0)$ to $r^{abc}(\omega)$. Although we assume there a dc field \mathbf{E}_{dc} rather than a mixing field $\mathbf{E}(\omega_0)$, the fact that the prefactors in the last two of Eqs. (A10) are identical

means that, again for $\hbar\omega_0$ much less than electronic energy scales but much larger than photon energies, \mathbf{E}_{dc} can be simply replaced by the mixing amplitude $\mathbf{E}(\omega_0)$ in the expressions we derive.

APPENDIX B: SECOND-ORDER OPTICAL RESPONSE

In this appendix we define the constituent terms given in Eq. (11) for both the SHG and LEO response functions. We note that all expressions explicitly satisfy intrinsic permutation symmetry.

For the SHG susceptibility the terms are

$$\chi_{II}^{abc}(-2\omega; \omega, \omega) = \frac{e^3}{\hbar^2} \sum_{nml} \int \frac{d\mathbf{k}}{4\pi^3} r_{nm}^a \{r_{ml}^b r_{ln}^c\} \left\{ \frac{2f_{nm}}{(\omega_{mn} - 2\omega)} + \frac{f_{ml}}{(\omega_{ml} - \omega)} + \frac{f_{ln}}{(\omega_{ln} - \omega)} \right\}, \quad (\text{B1})$$

$$\eta_{II}^{abc}(-2\omega; \omega, \omega) = \frac{e^3}{\hbar^2} \int \frac{d\mathbf{k}}{4\pi^3} \left\{ \sum_{nml} \omega_{mn} r_{nm}^a \{r_{ml}^b r_{ln}^c\} \left\{ \frac{f_{nl}}{\omega_{ln}^2 (\omega_{ln} - \omega)} - \frac{f_{lm}}{\omega_{ml}^2 (\omega_{ml} - \omega)} \right\} - 8i \sum_{nm} \frac{f_{nm} r_{nm}^a}{\omega_{mn}^2 (\omega_{mn} - 2\omega)} \{ \Delta_{mn}^b r_{mn}^c \} \right. \\ \left. + 2 \sum_{nml} \frac{f_{nm} r_{nm}^a \{r_{ml}^b r_{ln}^c\} (\omega_{ml} - \omega_{ln})}{\omega_{mn}^2 (\omega_{mn} - 2\omega)} \right\}, \quad (\text{B2})$$

$$\frac{i}{2\omega} \sigma_{II}^{abc}(-2\omega; \omega, \omega) = \frac{ie^3}{2\hbar^2} \int \frac{d\mathbf{k}}{4\pi^3} \left\{ \sum_{nml} \frac{f_{nm}}{\omega_{mn}^2 (\omega_{mn} - \omega)} [\omega_{nl} r_{lm}^a \{r_{mn}^b r_{nl}^c\} - \omega_{lm} r_{nl}^a \{r_{lm}^b r_{mn}^c\}] + \sum_{nm} \frac{f_{nm} \Delta_{nm}^a \{r_{mn}^b r_{nm}^c\}}{\omega_{mn}^2 (\omega_{mn} - \omega)} \right\}, \quad (\text{B3})$$

with all symbol definitions and conventions as detailed in Sec. II, and where

$$\Delta_{nm}^a(\mathbf{k}) \equiv v_{nn}^a(\mathbf{k}) - v_{mm}^a(\mathbf{k}). \quad (\text{B4})$$

For brevity, in the expression for $\chi^{abc}(-2\omega; \omega, \omega)$ we have written the \mathbf{r}_{nm} , Δ_{nm} , and ω_{nm} without the explicit \mathbf{k} dependence. The use of the curly brackets with the matrix elements implies a symmetrization with respect to the Cartesian components, $\{r_{ml}^b r_{ln}^c\} \equiv \frac{1}{2}(r_{ml}^b r_{ln}^c + r_{ml}^c r_{ln}^b)$.

For the LEO susceptibility, the constituent expressions are

$$\chi_{II}^{abc}(-\omega; \omega, 0) = \frac{e^3}{2\hbar^2} \sum_{nml} \int \frac{d\mathbf{k}}{4\pi^3} \left\{ \frac{f_{nm}}{(\omega_{mn} - \omega)} \left[\frac{r_{nm}^a r_{ml}^c r_{ln}^b}{\omega_{lm}} + \frac{r_{nm}^a r_{ml}^b r_{ln}^c}{\omega_{ln}} \right] + \left[\frac{f_{nl} r_{nm}^a r_{ml}^c r_{ln}^b}{(\omega_{ln} - \omega) \omega_{ml}} + \frac{f_{ml} r_{nm}^a r_{ml}^b r_{ln}^c}{(\omega_{ml} - \omega) \omega_{ln}} \right] \right\}, \quad (\text{B5})$$

$$\eta_{II}^{abc}(-\omega; \omega, 0) = \frac{ie^3}{2\hbar^2} \sum_{nm} \int \frac{d\mathbf{k}}{4\pi^3} \left\{ \frac{f_{nm} r_{nm}^a}{(\omega_{mn} - \omega)} \left[\frac{r_{mn}^c}{\omega_{mn}} \right]_{;c} + \frac{\partial}{\partial \omega} \left(\frac{f_{nm}}{2(\omega_{mn} - \omega)} (r_{nm}^a r_{nm}^b{}_{;b} - r_{nm}^a{}_{;b} r_{mn}^b) \right) \right\}, \quad (\text{B6})$$

$$\frac{i}{\omega} \sigma_{II}^{abc}(-\omega; \omega, 0) = \frac{ie^3}{2\hbar^2} \int \frac{d\mathbf{k}}{4\pi^3} \left\{ \frac{1}{2} \sum_{nm} \frac{f_{nm} \Delta_{nm}^a}{\omega_{mn}^2 (\omega_{mn} - \omega)} (r_{nm}^b r_{mn}^c - r_{nm}^c r_{mn}^b) - \sum_{nm} \frac{f_{nm}}{\omega_{mn} (\omega_{mn} - \omega)} r_{nm}^c{}_{;a} r_{mn}^b \right\}, \quad (\text{B7})$$

with the definitions

$$r_{mn;c}^b(\mathbf{k}) \equiv \frac{-[r_{mn}^b(\mathbf{k}) \Delta_{mn}^c(\mathbf{k}) + r_{mn}^c(\mathbf{k}) \Delta_{mn}^b(\mathbf{k})]}{\omega_{mn}(\mathbf{k})} - i \sum_p \frac{\omega_{mp}(\mathbf{k}) r_{mp}^b(\mathbf{k}) r_{pn}^c(\mathbf{k}) - \omega_{pn}(\mathbf{k}) r_{mp}^c(\mathbf{k}) r_{pn}^b(\mathbf{k})}{\omega_{mn}(\mathbf{k})}, \quad (\text{B8})$$

$$\left[\frac{r_{mn}^b(\mathbf{k})}{\omega_{mn}(\mathbf{k})} \right]_{;c} \equiv \frac{r_{mn;c}^b(\mathbf{k})}{\omega_{mn}(\mathbf{k})} + r_{mn}^b \frac{\partial}{\partial k^c} \left[\frac{1}{\omega_{mn}(\mathbf{k})} \right]. \quad (\text{B9})$$

Once again, we have not included the explicit \mathbf{k} dependence of the \mathbf{r}_{nm} , $\mathbf{\Delta}_{nm}$, and ω_{nm} in the expressions for $\chi^{abc}(-\omega; \omega, 0)$. All symbol definitions are identical to those used in the linear and SHG response functions.

APPENDIX C: LEO SUSCEPTIBILITY

In this appendix we detail the connection between $\chi^{abc}(-\omega; \omega, 0)$ and the usual electro-optic coefficient $r^{abc}(\omega)$. Proceeding with the nonlinear polarization leads, with linear response, to a total displacement vector

$$\begin{aligned} D^a(\omega) &= \sum_b \epsilon^{ab}(\omega) E^b(\omega) + 4\pi P_{\text{NL}}^a(\omega) \\ &= \sum_b \bar{\epsilon}^{ab}(\omega) E^b(\omega), \end{aligned} \quad (\text{C1})$$

where $\mathbf{P}_{\text{NL}}(\omega)$ is given by the last of Eqs. (A10), and the effective dielectric function

$$\bar{\epsilon}^{-ab}(\omega) = \epsilon^{ab}(\omega) + 8\pi \sum_c \chi^{abc}(-\omega; \omega, 0) E_{\text{dc}}^c. \quad (\text{C2})$$

Defining the impermeability tensor $\eta^{ab}(\omega)$ as the inverse of $\bar{\epsilon}^{ab}(\omega)$,

$$\sum_b \eta^{ab}(\omega) \bar{\epsilon}^{bc}(\omega) = \delta^{ac}, \quad (\text{C3})$$

and likewise for $\bar{\eta}^{ab}(\omega)$ and $\bar{\epsilon}^{ab}(\omega)$, the electro-optic coefficient relates the change in η^{ab} to the dc field,

$$\bar{\eta}^{ab}(\omega) = \eta^{ab}(\omega) + \sum_c r^{abc}(\omega) E_{\text{dc}}^c, \quad (\text{C4})$$

to first order. For crystal structures where ϵ^{ab} is diagonal, $\bar{\epsilon}^{ab}(\omega) = \delta^{ab} \epsilon(\omega)$, Eqs. (C2) and (C4) yield

$$\begin{aligned} \bar{\epsilon}^{ab}(\omega) &= \delta^{ab} \epsilon(\omega) + 8\pi \sum_c \chi^{abc}(-\omega; \omega, 0) E_{\text{dc}}^c, \\ \bar{\eta}^{ab}(\omega) &= \delta^{ab} \frac{1}{\epsilon(\omega)} + \sum_c r^{abc}(\omega) E_{\text{dc}}^c. \end{aligned} \quad (\text{C5})$$

The second of Eqs. (C5) seems to be the universally accepted definition of $r^{abc}(\omega)$ in the cgs units we are using at the moment. Since $\bar{\eta}^{ab}(\omega)$ is the inverse of $\bar{\epsilon}^{ab}(\omega)$ and these equations only hold to lowest order in \mathbf{E}_{dc} , we recover

$$\chi^{abc}(-\omega; \omega, 0) = -\frac{\epsilon^2(\omega) r^{abc}(\omega)}{8\pi}, \quad (\text{C6})$$

the desired relation. We note that the above expression is in cgs units. The equivalent expression in SI units is

$$\chi^{abc}(-\omega; \omega, 0) = -\frac{\epsilon_r^2(\omega) r^{abc}(\omega)}{2}, \quad (\text{C7})$$

the previously quoted result;⁶¹ $\epsilon_r(\omega)$ is the relative dielectric constant. If we make the approximation $\epsilon_r(\omega) = n^2(\omega)$, then Eq. (C7) becomes

$$\chi^{abc}(-\omega; \omega, 0) = -\frac{n^4(\omega) r^{abc}(\omega)}{2}, \quad (\text{C8})$$

where $n(\omega)$ is the index of refraction.

¹J. R. Chelikowsky and M. L. Cohen, Phys. Rev. B **14**, 556 (1976).
²C. S. Wang and B. M. Klein, Phys. Rev. B **24**, 3417 (1981).
³D. J. Moss, E. Ghahramani, J. E. Sipe, and H. M. van Driel, Phys. Rev. B **34**, 8758 (1986).
⁴S. Adachi, Phys. Rev. B **35**, 7454 (1987).
⁵M. Alouani, L. Brey, and N. E. Christensen, Phys. Rev. B **37**, 1167 (1988).
⁶Z. H. Levine and D. C. Allan, Phys. Rev. Lett. **63**, 1719 (1989).
⁷G. E. Engel and B. Farid, Phys. Rev. B **46**, 15 812 (1992).
⁸M.-Z. Huang and W. Y. Ching, Phys. Rev. B **47**, 9449 (1993).
⁹R. Del Sole and R. Girlanda, Phys. Rev. B **48**, 11 789 (1993).
¹⁰C.-C. Shih and A. Yariv, Phys. Rev. Lett. **44**, 281 (1980).
¹¹A. Hernandez-Cabrera, C. Tejedor, and F. Meseguer, J. Appl. Phys. **58**, 4666 (1985).
¹²S. Adachi, J. Appl. Phys. **72**, 3702 (1992).
¹³C. Y. Fong and Y. R. Shen, Phys. Rev. B **12**, 2325 (1975).
¹⁴H.-R. Ma, S. T. Chui, R. V. Kasowski, and W. Y. Hsu, Opt. Commun. **85**, 437 (1991).
¹⁵B. F. Levine, Phys. Rev. B **7**, 2600 (1973).
¹⁶M. M. Choy, S. Ciraci, and R. L. Byer, IEEE J. Quantum Electron. **11**, 40 (1975).
¹⁷Z. H. Levine and D. C. Allan, Phys. Rev. Lett. **66**, 41 (1991).

¹⁸Z. H. Levine and D. C. Allan, Phys. Rev. B **44**, 12 781 (1991).
¹⁹Z. H. Levine, Phys. Rev. B **49**, 4532 (1994).
²⁰M.-Z. Huang and W. Y. Ching, Phys. Rev. B **45**, 8738 (1992).
²¹M.-Z. Huang and W. Y. Ching, Phys. Rev. B **47**, 9464 (1993).
²²W. Y. Ching and M.-Z. Huang, Phys. Rev. B **47**, 9479 (1993).
²³D. J. Moss, J. E. Sipe, and H. M. van Driel, Phys. Rev. B **36**, 9708 (1987).
²⁴D. J. Moss, E. Ghahramani, J. E. Sipe, and H. M. van Driel, Phys. Rev. B **41**, 1542 (1990).
²⁵E. Ghahramani, D. J. Moss, and J. E. Sipe, Phys. Rev. B **43**, 8990 (1991).
²⁶E. Ghahramani, D. J. Moss, and J. E. Sipe, Phys. Rev. B **43**, 9700 (1991).
²⁷D. J. Moss, E. Ghahramani, and J. E. Sipe, Phys. Status Solidi B **164**, 587 (1991).
²⁸J. E. Sipe and E. Ghahramani, Phys. Rev. B **48**, 11 705 (1993).
²⁹C. Aversa and J. E. Sipe, Phys. Rev. B **52**, 14 636 (1995).
³⁰A. Dal Corso and F. Mauri, Phys. Rev. B **50**, 5756 (1994).
³¹H. Krakauer, M. Posternak, and A. J. Freeman, Phys. Rev. B **19**, 1706 (1979).
³²E. Wimmer, H. Krakauer, M. Weinert, and A. J. Freeman, Phys. Rev. B **24**, 864 (1981).
³³R. W. Boyd, *Nonlinear Optics* (Academic, San Diego, 1992).

- ³⁴J. P. Perdew and M. Levy, Phys. Rev. Lett. **51**, 1884 (1983).
- ³⁵L. J. Sham and M. Schluter, Phys. Rev. Lett. **51**, 1888 (1983).
- ³⁶M. S. Hybertsen and S. G. Louie, Phys. Rev. Lett. **55**, 1418 (1985).
- ³⁷M. S. Hybertsen and S. G. Louie, Phys. Rev. B **34**, 5390 (1986).
- ³⁸S. B. Zhang *et al.*, Phys. Rev. B **40**, 3162 (1989).
- ³⁹S. J. Jenkins, G. P. Srivastava, and J. C. Inkson, Phys. Rev. B **48**, 4388 (1993).
- ⁴⁰G. E. Engel, B. Farid, C. M. M. Nex, and N. H. March, Phys. Rev. B **44**, 13 356 (1991).
- ⁴¹R. Del Sole, L. Reining, and R. W. Godby, Phys. Rev. B **49**, 8024 (1994).
- ⁴²W. G. Aulbur, L. Jonsson, and J. W. Wilkins (unpublished).
- ⁴³X. Gonze, P. Ghosez, and R. W. Godby, Phys. Rev. Lett. **74**, 4035 (1995).
- ⁴⁴Z. H. Levine and D. C. Allan, Phys. Rev. B **43**, 4187 (1991).
- ⁴⁵J. Chen, Z. H. Levine, and J. W. Wilkins, Phys. Rev. B **50**, 11 514 (1994).
- ⁴⁶C. Flytzanis, in *Quantum Electronics*, edited by H. Rabin and C. L. Tang (Academic, New York, 1975), Vol. IA, p. 9.
- ⁴⁷J. Rath and A. J. Freeman, Phys. Rev. B **11**, 2109 (1975).
- ⁴⁸G. Lehmann and M. Taut, Phys. Status Solidi B **54**, 469 (1972).
- ⁴⁹D. J. Moss, J. E. Sipe, and H. M. van Driel, Phys. Rev. B **36**, 1153 (1987).
- ⁵⁰H. R. Philipp and H. Ehrenreich, Phys. Rev. **129**, 1550 (1963).
- ⁵¹D. E. Aspnes and A. A. Studna, Phys. Rev. B **27**, 985 (1983).
- ⁵²S. Adachi, *GaAs and Related Materials: Bulk Semiconducting and Superlattice Properties* (World Scientific, Teaneck, NJ, 1994).
- ⁵³P. Lautenschlager, M. Garriga, S. Logothetidis, and M. Cardona, Phys. Rev. B **35**, 9174 (1987).
- ⁵⁴E. Ghahramani, Ph.D. thesis, University of Toronto, 1990.
- ⁵⁵E. D. Palik, in *Handbook of Optical Constants of Solids*, edited by E. D. Palik (Academic, New York, 1985), p. 429.
- ⁵⁶A. Borghesi and G. Guizzetti, in *Handbook of Optical Constants of Solids*, edited by E. D. Palik (Academic, New York, 1985), p. 445.
- ⁵⁷E. Ghahramani and J. E. Sipe, Appl. Phys. Lett. **64**, 2421 (1994).
- ⁵⁸D. A. Roberts, IEEE J. Quantum Electron. **28**, 2057 (1992).
- ⁵⁹B. F. Levine and C. G. Bethea, Appl. Phys. Lett. **20**, 272 (1972).
- ⁶⁰R. C. Miller, Appl. Phys. Lett. **5**, 17 (1964).
- ⁶¹I. P. Kaminow and E. H. Turner, *Handbook of Lasers* (Chemical Rubber, Cleveland, OH, 1971), p. 447.
- ⁶²F. G. Parsons and R. K. Chang, Opt. Commun. **3**, 173 (1971).
- ⁶³D. Bethune, A. J. Schmidt, and Y. R. Shen, Phys. Rev. B **11**, 3867 (1975).
- ⁶⁴R. K. Chang, J. Ducuing, and N. Bloembergen, Phys. Rev. Lett. **15**, 415 (1965).
- ⁶⁵C. A. Berseth, C. Wuethrich, and F. K. Reinhart, J. Appl. Phys. **71**, 2821 (1992).
- ⁶⁶Y. V. Shalidin and D. A. Belogurov, Kvant. Elektron. (Moscow) **3**, 1660 (1976) [Sov. J. Quantum Electron. **6**, 897 (1976)].
- ⁶⁷T. E. Walsh, RCA Rev. **27**, 323 (1966).
- ⁶⁸N. Suzuki and K. Tada, Jpn. J. Appl. Phys. **23**, 291 (1984).
- ⁶⁹N. Suzuki and K. Tada, Jpn. J. Appl. Phys. **23**, 1011 (1984).
- ⁷⁰J. Faist and F. K. Reinhart, J. Appl. Phys. **67**, 7006 (1990).
- ⁷¹M. Sugie and K. Tada, Jpn. J. Appl. Phys. **15**, 421 (1976).
- ⁷²A. Yariv, C. A. Mead, and J. V. Parker, IEEE J. Quantum Electron. **2**, 243 (1966).
- ⁷³W. D. Johnston, Jr. and I. P. Kaminow, Phys. Rev. **188**, 1209 (1969).
- ⁷⁴I. P. Kaminow, IEEE J. Quantum Electron. **4**, 23 (1968).
- ⁷⁵G. L. Herrit and H. E. Reedy, in *Optical Materials: Processing and Science*, edited by D. B. Poker and C. Ortiz, MRS Symposia Proceedings No. 152 (Materials Research Society, Pittsburgh, 1989), p. 169.
- ⁷⁶D. F. Nelson and E. H. Turner, J. Appl. Phys. **39**, 3337 (1968).
- ⁷⁷Y. Berozashvili, S. Machavariani, A. Natsvlishvili, and A. Chirakadze, J. Phys. D **22**, 682 (1989).